J. Electrochem. Sci. Eng. **15(1)** (2025) 2501; http://dx.doi.org/10.5599/jese.2501

Open Access : : ISSN 1847-9286
www.jESE-online.org

Original scientific paper

Polymer-modified screen-printed electrode-based electrochemical sensors for doxorubicin detection

Iva Dimitrievska✉, Perica Paunović and Anita Grozdanov

Ss. Cyril and Methodius University in Skopje, Faculty of Technology and Metallurgy, Rugjer Boshković 16, 1000 Skopje, North Macedonia

Corresponding author: ✉*iva@tmf.ukim.edu.mk*

Received: October 1, 2024; Accepted: November 27, 2024; Published: December 4, 2024

Abstract

In the last decade, intensive research has been performed in the field of analytical electrochemistry, seeking designs of electrochemical sensors capable of providing better analytical characteristics in terms of sensitivity, selectivity, reliability, ease of fabrication and use, and low cost, especially for pharmaceutical drug monitoring. Our research has primarily focused on developing screen-printed electrode-based sensors and their application as electrochemical platforms for drug determination and monitoring, specifically emphasizing their suitability for surface modification. A commercial screen-printed graphene electrode was used as the electrochemical sensing component, which was subsequently modified with polymers, such as polyvinylidene fluoride and chitosan. All studied electrodes were tested using a doxorubicin hydrochloride (DOX) solution with a concentration of 0.002 mol L^{-1} dissolved in 0.1 mol L^{-1} phosphate-buffered saline at pH 6.7. Cyclic voltammetry was used as an electrochemical characterization technique to gather data on all tested electrodes' electrochemical activity. The morphological characterization of the electrodes was done using scanning electron microscopy. The changes in the electrolyte during the electrochemical measurements were followed through ultraviolet-visible spectroscopy. The modified electrodes demonstrated a favorable electrochemical response to DOX and exhibited higher electrical conductivity than the commercial one. The characterization results indicated that the Ch-modified electrode exhibited excellent electrochemical conductivity and demonstrated strong electrochemical performance. The evaluations of this electrode comprised the definition of the lowest limit of detection and limit of quantification among the tested electrodes, with values of 9.822 and 32.741 µmol L^{-1}, respectively, within a linear concentration range from 1.5 to 7.4 µmol L^{-1}. Additionally, the electrodes showed excellent repeatability, stability, and reproducibility, confirming their suitability for sensitive DOX detection.

Keywords

Graphene; polyvinylidene fluoride; chitosan; anticancer medication, sensing

Introduction

Doxorubicin hydrochloride (DOX) is a potent and widely used anticancer medication in the anthracyclines class. Commonly referred to as the “golden standard”, DOX is highly effective against a broad

spectrum of malignancies, including breast cancer, lymphomas, leukemias, and sarcomas. DOX's anticancer and antitumor mechanism of action is related to the inhibition of DNA replication and transcription processes through intercalation between base pairs, thereby leading to cell death [1]. Additionally, it can generate cytotoxic reactive oxygen species, leading to oxidative stress and induction of apoptosis, effectively targeting rapidly dividing cancer cells and exerting cellular damage [2].

Despite its remarkable efficiency, DOX has limitations because of its severe acute and long-term side effects. One major concern is raised regarding its dose-dependent cardiotoxicity, which can lead to irreversible damage to the heart muscle and potentially compromise the long-term health of cancer survivors [3]. Therefore, monitoring and keeping the DOX concentration under control in patients following cancer treatment is critical to minimize the side effects during clinical trials, assess toxicity, and follow the therapeutic efficiency.

Numerous analytical methods have already been reported for DOX determination and monitoring, using techniques such as high-performance liquid chromatography (HPLC), liquid chromatography coupled with mass spectroscopy (LC-MS), ultraviolet-visible spectroscopy (UV-Vis), fluorescence, *etc*. [4-15]. Although HPLC and LC/MS methods present the highest selectivity and sensitivity towards pharmaceutical molecules, all these techniques demand complicated and time-consuming sample preparation, making them unsuitable for rapid detection. Electrochemical methods receive much consideration due to their ease of use, inexpensive equipment, simple and fast manipulation, and real-time sensing. Electrochemical sensors have been reported as one of the most favorable and practical methods for pharmaceutical compound detection in human blood samples, offering unique advantages such as miniaturization, portability, rapid response, and satisfactory selectivity and sensitivity [16]. Implementing nanotechnology to conventional electrochemical sensors results in enhanced sensing mechanisms due to nanomaterials' superior properties. Electrochemical sensors based on nanomaterials show incredible performance due to their large specific surface area and high reactivity, making them a highly popular topic among researchers.

Researchers continuously work towards improving the surface kinetics of electrodes to design electrochemical sensors with advanced performance and satisfactory results. Extensive research has been focused on screen-printed electrode (SPE) based sensors as electrochemical sensors for drug determination, particularly suitable for surface modification. Carbon nanomaterials (graphene, carbon nanotubes, carbon nanorods, carbon nanoflakes, *etc.*) are the most widely used nanostructures as electrode modifiers and an excellent choice for electrochemical sensor performance improvement [17]. Graphene is suitable for electrochemical sensing applications because of its dimensions and improvement of the overall sensitivity when increasing the number of surface electroactive centers and enhancing the rate of electron transfer [18]. Moreover, polymeric modification by coating onto electrode surfaces offers significant flexibility. Polymers contain diverse functional groups, allowing for exceptional high surface coverage through thick multilayer coating [19]. Some commonly used polymers are chitosan (CH) and polyvinylidene fluoride (PVDF). Chitosan, a natural biopolymer, is a highly biocompatible amino saccharide, which can also be considered environmentally friendly due to its low toxicity [20,21]. Chitosan's surface can be chemically modified with many functional groups, allowing chitosan-modified sensors to interact with the target analyte, such as DOX (Figure 1). There are active amino groups in the chitosan's structure, allowing the attachment of the functional groups of other analytes. The amino groups are also determining the chitosan's cationic nature. Moreover, using chitosan nanoforms enhances the sensing platform [21]. PVDF is a highly non-reactive thermoplastic fluoropolymer known for its superior chemical resistance, versatility, and robustness, among other exceptional properties [22]. PVDF is a highly hydrophobic polymer,

allowing the analytes to adsorb on its surface through van der Waals forces and hydrophobic interactions. A unique combination of physicochemical characteristics has led to PVDF's significant use in a wide range of applications. Over time, PVDF has emerged as the most extensively used material in electrochemical applications, where attributes such as high sensitivity, stability, and rapid response are needed [23].

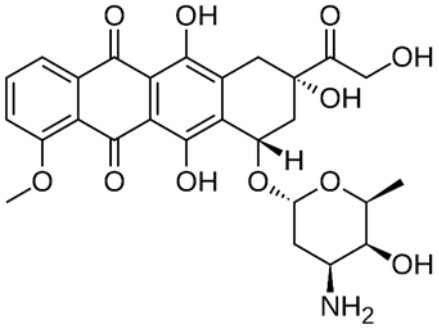

Figure 1. Chemical structure of doxorubicin hydrochloride

The aforementioned materials are extensively used for sensor development, as reported in the literature. Zhao *et al.* [24] developed an electrochemical sensor for the sensitive detection of DOX based on a novel synthesized electrode material that includes gold nanoparticles and multiwalled carbon nanotubes decorated with a covalent organic framework used for glassy carbon electrode modification. The designed sensor showed improved distribution of electroactive sites and higher affinity towards DOX, contributing to enhanced electrocatalytic sensor activity. The authors reported an improved linear range for DOX from 0.08 to 25 µmol L^{-1} with a low detection limit of 16 nmol L^{-1} in spiked human serum and cell lysate samples. A novel, two-dimensional nanocomposite with a mediator role in DOX's detection has been proposed by Mehmandoust *et al.* [25]. The synthesized nanocomposite based on two-dimensional graphitic carbon nitride/sodium dodecyl sulfate/graphene nanoplatelets has been used for surface modification of screen-printed electrodes. The authors reported excellent electrochemical performance of the sensor, including a wide dynamic linear range from 0.03 to 1.0 µmol L^{-1} and 1.0 to 13.5 µmol L^{-1} with a low detection limit of 10.0 nmol L^{-1}. Upon testing, the developed sensor showed excellent sensitivity, stability, good reproducibility, and repeatability toward DOX detection in real human plasma and urine samples, with correlation and variation coefficients below 6.0 %.

An electrochemical sensor designed using tryptophan/(polyethylene glycol)ylated-$CoFe_2O_4$ nanoparticles to modify glassy carbon electrodes for sensing DOX in clinical fluids has been proposed by Abbasi *et al.* [26]. Under optimized conditions, the proposed sensor exhibits a low quantification limit of 30 ng mL^{-1} and dynamic linear limits from 30 ng mL^{-1} to 1.0 µg and 1.0 to 5.0 µg mL^{-1}, respectively. Guo *et al.* [27] synthesized ternary nanocomposites with silver nanoparticles (AgNPs), carbon dots (CDs), and reduced graphene oxide (rGO), which were electrodeposited on a glass carbon electrode (GCE) and reported superior electrocatalytic activities for DOX reduction. They reported superior electrocatalytic activities for DOX reduction in the range from 0.01 to 2.5 µmol L^{-1} (R^2 = 0.9956), and a low detection limit of 2 nmol L^{-1}. An electrochemical device based on a screen-printed diamond electrode (SPDE) for a single drop quantification of DOX has been reported by Stanković *et al.* [28]. The authors observed high electroactivity over a wide range of pHs and a working linear range for DOX from 0.1 to 2.5 µmol L^{-1}.

Behravan *et al.* [29] developed an electrochemical sensor based on reduced graphene oxide (rGO)/ /gold (Au) nanoparticles/polypyrrole (PPy)/nanocomposite-modified glassy carbon electrode (GCE) for the detection of DOX. The optimization process determined pH 5.5 to be the optimal value. The

authors reported a high sensitivity of 185 μA $mmol^{-1}$ L, a low detection limit of 0.02 μmol L^{-1}, a wide linear range of 0.02 μmol L^{-1} to 25 mmol L^{-1}, and excellent reproducibility and stability properties. Carbon dots/cerium oxide (CDs/CeO_2) nanocomposites modified screen-printed carbon electrode has been developed by Thakurb *et al.* [30] for sensitive detection of DOX. The nanocomposite consisting of 5 wt.% CDs (CDs-5.0/CeO_2) was reported to have the highest oxidation response to DOX (20 μmol L^{-1}) in a solution with a pH of 5. Moreover, the authors reported a linear concentration range of 0.2 to 20 μmol L^{-1} and a low detection limit of 0.09 μmol L^{-1}. In addition to this, the modified sensor showed superior selectivity and sensitivity towards DOX. Other authors, Abhishek Singh *et al.* [31], also reported the use of carbon dots-based electrochemical sensors based on screen-printed carbon electrodes, but their nanocomposites consisted of carbon dots and magnesium oxide (CDs/MgO). They reported that the modification with 5 wt.% CDs (CDs-5.0/MgO) exhibited the highest oxidation response for DOX (10 μmol L^{-1}) at pH 5 and a scan rate of 50 mV s^{-1}. The testing was done in a linear concentration range of 0.1 to 1 μmol L^{-1} and a low detection limit of 0.09 μmol L^{-1}. The proposed sensor showed superior selectivity towards DOX upon testing the effect of the common interfering agents.

Sun *et al.* [32] developed a new acetylene black (AB) glassy carbon electrode (GCE) for the detection of DOX in human serum. The authors report detailed optimization of scanning rate, AB volume, concentration, DOX enrichment time, and pH as the main parameters that affect electrochemical detection. The oxidative peak current has been reported to be linearly proportional to DOX's concentration in the ranges of 0.01 to 2.5 μmol L^{-1}, with a detection limit of 3.006 nmol L^{-1}. The method was found to be implemented for quantitative analysis of spiked samples of human serum with a satisfactory recovery from 91.22 to 101.34 %. Gold nanoparticles decorated-multi-walled carbon nanotubes (MWCNTs) have been used as an ultrasensitive electrochemical sensor by Sharifi *et al.* [33] for the detection of DOX. The authors report an efficient electrocatalytic reduction activity of DOX, which leads to a peak current density increase and a reduction in over-potential decrease. The modified electrode has demonstrated a wide linear concentration range from 10^{-5} to 1 μmol L^{-1}, with a low limit of detection (6.5 pmol L^{-1}). The developed sensor exhibited appropriate selectivity, reproducibility, repeatability, and long-term stability.

Alavi-Tabari *et al.* [34] worked on the simultaneous detection of DOX and dasatinib (DAS) using a ZnO nanoparticle/1-butyl-3-methylimidazolium tetrafluoroborate modified carbon paste electrode (ZnO-NPs/BMTFB/ /CPE). The modified electrode has been reported to exhibit a good oxidation response of DOX in a linear concentration range of 0.07 to 500 μmol L^{-1}. The limit of detection was reported to be 9.0 nmol L^{-1}. An electrochemical sensor for simultaneous detection of DOX and methotrexate (MTX) using carbon black (CB), cooper nanoparticles (CuNPs), and Nafion-modified glassy carbon electrode (CuNPs-CB-Nafion/GCE) has been reported by Materon *et al.* [35]. Under optimized conditions, the modified electrode showed a linear response range of 0.45 to 5.1 μmol L^{-1}, with a limit of detection of 24 nmol L^{-1}. The authors demonstrated a successful application of the sensor to determine DOX and MTX in human urine and water river samples, with a spike recovery of nearly 100 % under optimized conditions.

As a novel DOX sensor, Rahimi *et al.* [36] designed a modified screen-printed electrode with a bird nest-like nanostructured NiCo2O4 (BNNS-$NiCo_2O_4$/SPE). Their sensor exhibited a linear concentration range between 0.01 and 600.0 μmol L^{-1}, with a detection limit of 9.4 nmol L^{-1}. Graphene quantum dot (GQD)-modified glassy carbon electrode for determination of DOX has been investigated by Hashemzadeh *et al.* [37]. The authors determined a substantial decrease in the overvoltage (-0.56 V) of the oxidation reaction of DOX at low potential compared to ordinary electrodes. A wide linear concentration range of the modified electrode was reported from 0.018 to 3.600 μM, with a suitable

limit of detection of 0.016 µmol L^{-1} and a limit of quantification of 0.050 µmol L^{-1}. The developed sensor has good linearity (R^2 = 0.9971), inter-day precision (3.33 % RSD), intra-day precision (5.03 % RSD), and accuracy. Mohammadi *et al.* [38] fabricated a sensor based on Ni-Fe layered double hydroxide (Ni-Fe LDH)-modified screen-printed electrode (Ni-Fe LDH/SPE) for the detection of DOX and DAS. The proposed sensor exhibited a broad linear concentration range from 0.04 to 585.0 µmol L^{-1}, with a narrow limit of detection of 0.01 µmol L^{-1}. The authors confirmed the practical application of the developed sensor by sensing DOX and DAS in biological matrices.

An electrochemical sensor based on screen-printed electrodes for simultaneous detection of DOX and simvastatin (SMV) has been published by Rus *et al.* [39]. Different materials such as graphite, gold nanoparticles-decorated graphite, gold, platinum, and pencil graphite. have been implemented as working electrodes. The authors reported that the use of amperometry allowed for a better limit of detection (0.1 µg mL^{-1} for DOX) than the one obtained in voltammetry (1.5 µg mL^{-1}). The limit of quantification using amperometry was 0.5 µg mL^{-1} in the dynamic concentration range of 0.5 to 65 µg mL^{-1}, while using voltammetry was 1 µg mL^{-1} in the dynamic range from 1 to 100 µg mL^{-1}. The authors concluded that the graphite electrodes showed the highest oxidation peak intensity for DOX and that the oxidation is reversible, involving the exchange of two protons and two electrons.

Wang *et al.* [40] demonstrated the use of electrochemically pretreated glassy carbon electrodes (p-GCE) modified with vertically ordered mesoporous silica films (VMSF) for determination of DOX. The authors emphasize the pretreatment process as a simple and cost-effective way to improve the catalytic properties on the interface, allowing for stable growth of VMSF without using adhesive layers. The proposed sensor exhibits ultrahigh sensitivity of 23.94 µA $µM^{-1}$, a low detection limit of 0.2 nmol L^{-1}, along with a wide linear concentration range from 0.5 nmol L^{-1} to 23 µmol L^{-1}. An electrochemical sensor based on a cyclodextrin-graphene hybrid nanosheet-modified glassy carbon electrode (CD-GNs/GCE) has been reported by Guo *et al.* [41] for the detection of DOX and MTX. The linear response range under optimized conditions of the proposed sensor was 10 nmol L^{-1} to 0.2 µmol L^{-1}, with a detection limit of 0.1 nmol L^{-1}. Another sensor based on vertically ordered mesoporous silica films (VMSFs) and N-doped graphene quantum dots (NGQDs)-modified indium tin oxide (ITO) has been proposed by Zhang *et al.* [42]. The proposed sensor resulted in good analytical performance, such as a wide linear range (5 nmol L^{-1} to 0.1 µmol L^{-1} and 0.1 to 1 µmol L^{-1}), high sensitivity (30.4 µA $µmol^{-1}$ L), and a low limit of detection (0.5 nmol L^{-1}). The authors reported good selectivity and recoveries of 97.0 to 109 % upon testing the modified sensor in human serum and urine samples.

Haghshenas *et al.* [43] fabricated an oxidized multiwalled carbon nanotube/glassy carbon electrode (OMWCNT/GCE)-based sensor used for simultaneous detection of dopamine (DA) and DOX. Under optimal conditions, the modified electrode operated in the concentration range of 0.04 to 90 µmol L^{-1}, with a detection limit of 9.4 nmol L^{-1}. The authors successfully demonstrated the practical application of the modified electrode in human blood serum and urine samples. A nano-titania (nano-TiO_2)/Nafion composite film-modified GCE has been synthesized and developed by Fei *et al.* [44]. The modified electrode greatly enhanced the reduction of DOX compared to the bare GCE. The authors reported a linear response of DOX in the range from 5.0 nmol L^{-1} to 2.0 µmol L^{-1}, with a detection limit of 1.0 nmol L^{-1}. The RSD of the inter-electrode is reported as 5.1 %, indicating the reproducibility of the method. The stability of the modified electrode was tested after 2-week air exposure, with a decrease of only 3.8 % in the initial response. The recovery of the modified electrode ranged from 94.9 to 104.4 % in human plasma samples. A DOX sensor based on multiwalled carbon nanotubes (MWCNTs) and spinel-structured cobalt ferrite ($CoFe_2O_4$) magnetic nanoparticles (MNPs)-modified carbon paste

electrode has been developed by Taei *et al.* [45]. The proposed sensor under optimized conditions is characterized by a concentration range of 0.05 to 1150 nM, and a low detection limit of 10 pM.

Electrochemical sensors have seen various innovations, as highlighted by recent studies [46-52]. The literature review conducted for this research focuses on implementing a specific and unique combination of materials tailored for DOX detection. Although all these studies valuably contribute to the field, none investigate the approach proposed in this manuscript: a polymer-modified screen-printed electrode as a sensing substrate designed for sensitive and repeatable DOX detection. Our simple, cost-effective modification offers improved sensitivity and is optimized specifically for targeted DOX applications. The advantages of our developed sensor underscore the originality of our approach, presenting a novel and practical pathway in the electrochemical detection of pharmaceuticals.

In this study, we investigated graphene-based screen-printed electrodes (SPEs) modified with polymers for the detection of DOX in a simulated biological matrix. The bare graphene SPEs were surface-modified using chitosan and polyvinylidene fluoride (PVDF) and their electrochemical performance was compared to that of commercial graphene SPEs. This paper presents a comparative analysis of the electrochemical and physical properties of the polymer-modified graphene SPEs, aiming to develop a simple electrochemical sensor for detecting clinical concentrations of DOX.

Experimental

Commercially available SPEs, based on graphene (G) (model DS1100) were purchased from Dropsens Ltd, Llanera, Asturias, Spain, and further modified with polymeric coatings.

All chemicals used were of analytical grade and used without further purification. Biocompatible natural polymer chitosan (Ch) and electroactive polymer polyvinylidene fluoride (PVDF), purchased from Sigma Aldrich, were used as electrode modifiers. PVDF was dissolved in N,N-dimethylacetamide at 2 wt.% concentration, deposited onto the surface of the commercial graphene SPE, and allowed to dry at room temperature. The same preparation method was used for the chitosan 2 wt.% solution.

Doxorubicin hydrochloride was purchased as Adrimisin®, Saba (2 mg mL^{-1}) from a local pharmacy. The pure powdered active pharmaceutical ingredient was dissolved in distilled water to a concentration of 0.01 mol L^{-1}. 0.1 mol L^{-1} phosphate buffer saline (PBS) was prepared following the method given in European Pharmacopoeia 11.0 (4014300), using sodium dihydrogen phosphate and disodium hydrogen phosphate dihydrate. The PBS was adjusted to pH 6.7 to simulate the normal human blood pH range. The electrolyte for the electrochemical measurements was prepared by adding a corresponding amount of the dissolved DOX solution to 20 mL of PBS, with a final concentration of 0.002 mol L^{-1}. A calibration curve constructed from 1.5 to 7.4 µmol L^{-1} was used to estimate the limit of detection (LOD) and quantification (LOQ). LOD and LOQ were calculated based on S/N = 3 and S/N = 10, respectively. All electrochemical measurements were performed in triplicate at 25 °C by immersing the SPEs in the electrolyte solution. Figure 4 shows good contact between the solution and the three-electrode system.

The electrochemical behavior of the modified electrodes towards DOX was investigated by cyclic voltammetry (CV). The experimental setup of the electrochemical measurements is shown in Figure 2. All CV measurements were obtained in the potential range from -0.05 to +0.6 V, under automatic current, with 5 scans. Various scan rates (20, 50, 100, 200, and 300 mV s^{-1}) were employed for the determination of the electroanalytical parameters related to the DOX's oxidation/reduction processes: the rate-determining step (adsorption or diffusion), electrochemical mechanism (Tafel's

slope *b*, charge transfer coefficient *α*, and number of transferred electrons *n*), and double-layer capacitance C_{dl}. After an optimization process, the scan rate range was carefully chosen to balance the sensitivity and stability of the redox signals for DOX. Lower scan rates (*e.g.,* 10 mV s^{-1}) could result in a prolonged analysis and might increase the potential for adsorptive interference, while higher scan rates (*e.g.,* 400 mV s^{-1}) may cause peak broadening or shift due to kinetic limitations and potential electrode surface effects. Thus, the chosen range provides robust, reproducible data while maintaining adequate signal clarity. The measurements were performed at room temperature, using the potentiostat/galvanostat SPELEC "Dropsens", Spain, operated with the Dropview software.

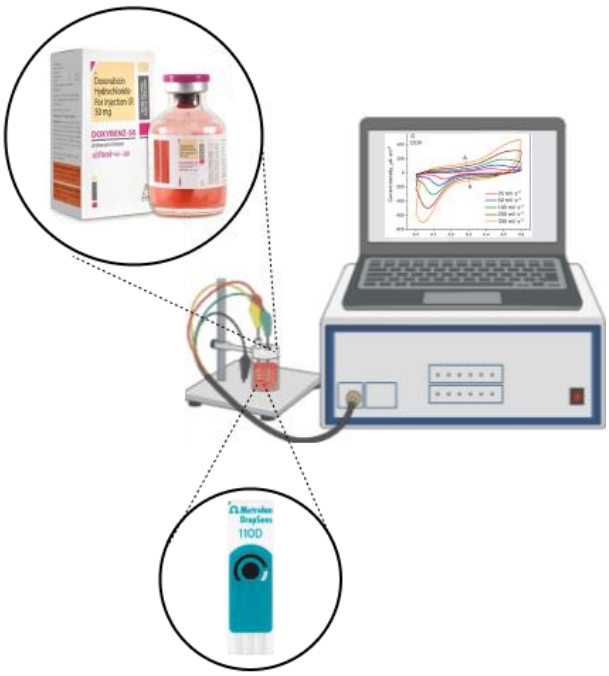

Figure 2. *Experimental setup of the electrochemical measurements*

Physical characterization of the SPEs was performed by scanning electron microscopy (SEM). The surface morphology of the SPEs was analyzed with FEI Quanta 2000 SEM, using a secondary electron detector and acceleration voltage of 30 kV, under a high vacuum. Before and after CV measurements, the electrolyte was investigated using UV-Vis spectroscopy. UV-Vis measurements were conducted using a Spectroquant Prove 600 spectrophotometer within a wavelength scan range of 200-800 nm.

Results and discussion

Electrochemical detection of doxorubicin hydrochloride

The electrochemical profile of the modified SPEs and their sensitivity towards DOX were followed by CV in 0.1 mol L^{-1} PBS with pH 6.7. Three SPE systems were investigated, including commercial graphene (G), chitosan-modified graphene (G/Ch), and PVDF-modified graphene SPE (G/PVDF). The characteristic cyclic voltammograms of the tested electrodes, in 0.1 mol L^{-1} PBS and 0.002 mol L^{-1} DOX solution, are shown in Figure 3a and 3b, respectively. Additionally, Figures 3c, 3d, and 3e display the individual voltammograms as a correlation between the current density (*j*) and the potential (*E*), along with the calculated values for the oxidation peak potential ($P_{ox.}$), reduction peak potential ($P_{red.}$), and peak-to-peak separation potential (ΔE_p). All voltammograms were scanned in the potential range of -0.05 to 0.6 V at a scan rate of 25 mV s^{-1}.

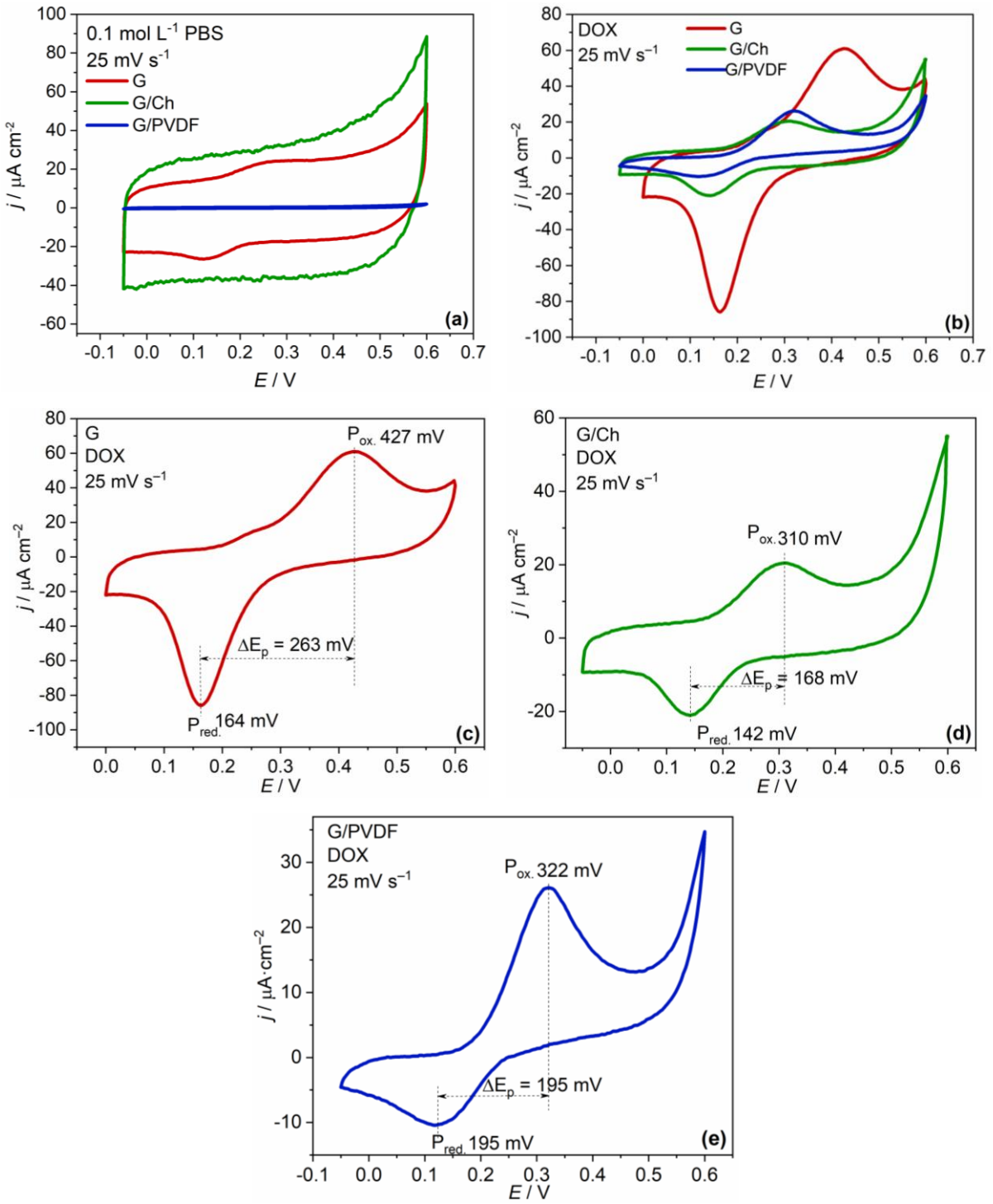

Figure 3. *Electrochemical detection of DOX. Tested SPEs' cyclic voltammograms comparison in (a) 0.1 mol L^{-1} PBS and (b) 0.002 mol L^{-1} DOX solution. Electrochemical parameters were calculated for (c) commercial graphene electrode; (d) chitosan-modified electrode and (e) PVDF-modified electrode in 0.002 mol L^{-1} DOX solution.*

The voltammograms in Figure 3a correspond to the measurements done in 0.1 mol L^{-1} PBS solution. The absence of peaks in PBS suggests that the electrolyte solution does not contain redox-active species under the applied experimental conditions. PBS, being a buffer, is commonly used as a background electrolyte because it does not contain electroactive compounds that undergo oxidation or reduction at the applied potential range. The lack of peaks confirms that the SPEs exhibit minimal background current in PBS, ensuring a stable measurement baseline and a clear

distinction between the background response and any electrochemical signals that may appear upon adding an analyte, such as DOX.

Two characteristic current peaks are observed in the electrochemical spectrum of the tested SPEs in the 0.002 mol L^{-1} DOX solution (Figure 3b), originating from the analyte. The peak labeled as $P_{ox.}$ in the anodic region of the voltammogram corresponds to DOX's oxidation, while the peak labeled $P_{red.}$ in the cathodic region corresponds to DOX's reverse reaction of reduction. This indicates a reversible reaction on the electrode surface, which can proceed in both directions, as shown in Figure 4 [53].

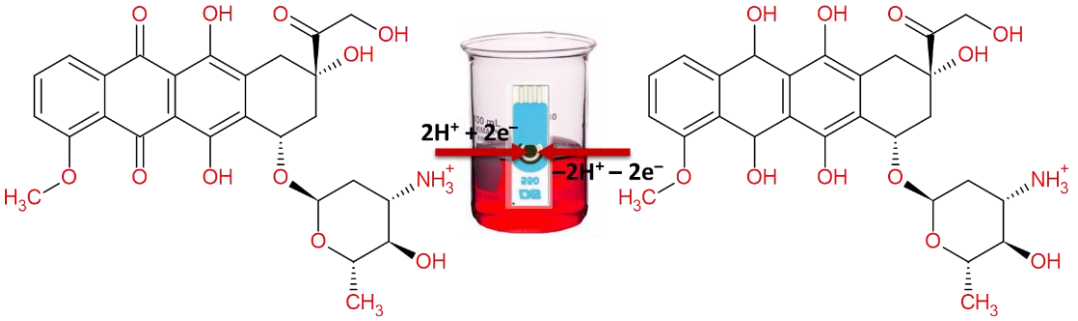

Figure 4. *Electrochemical oxidation of doxorubicin*

The reversibility of this reaction is contingent upon the electrode in which it takes place. The reaction is fully reversible when the oxidation (Pox.) and reduction (Pred.) peaks are situated at the same potential and exhibit equal intensities. Conversely, if the peak potentials are disparate and their intensities vary, the reversibility is substantially reduced.

Upon comparing the obtained voltammograms, it is evident that the commercial graphene SPE (G) exhibits the strongest current response, which is expected according to the literature and may be ascribed to the superior conductivity and large surface area of graphene [54,55]. The commercial graphene SPE exhibited the most prominent anodic peak, attributed to its electrocatalytic effect and higher background current [56]. In addition, the oxidation ($P_{ox.}$) peaked at 427 mV, surpassing the values of other modified electrodes by over 100 mV. Moreover, the potential difference between the anodic (oxidation) and cathodic (reduction) peaks, also known as peak-to-peak separation potential (ΔE_p), showed a significant increase compared to other systems, reaching 263 mV. This indicates that the DOX oxidation reaction on the commercial graphene SPE is less reversible [57-59]. The polymer-modified graphene SPEs with chitosan (G/Ch) and polyvinylidene fluoride (G/PVDF), demonstrate satisfactory electrochemical responses in comparison to the commercial graphene electrode. The intensified current density of the peaks ($j_{P_{ox.}}$ = 20.5 µA cm^{-2} for G/Ch and $j_{P_{ox.}}$ = 26 µA cm^{-2} for G/PVDF), lower potentials at which they appear ($E_{P_{ox.}}$ = 310 mV for G/Ch and $E_{P_{ox.}}$ = 322 mV for G/PVDF), and smaller peak-to-peak separation potentials (ΔE_p = 168 mV for G/Ch and ΔE_p = 195 mV for G/PVDF) indicate a faster and more reversible electron exchange in the redox reaction shown in Figure 4 [57]. This is mainly attributed to the strong interaction of DOX with G/Ch and G/PVDF. DOX, having an aromatic structure, can interact with graphene through π-π and hydrophobic interactions, chitosan through hydrophobic and electrostatic interactions, and PVDF through surface adsorption [57,60,61]. The interaction mechanism between the surface-modified electrodes and DOX typically relies on functional groups' reactions through hydrogen bonding, van der Waals forces, and hydrophobic interactions.

After comparing the modified sensor electrodes, it can be concluded that the G/PVDF system exhibits a slightly stronger current response over the G/Ch system (26 compared to 20.5 µA cm^{-2}). Conversely, the G/Ch system has the advantage of a lower potential for the oxidation reaction of

DOX (310 mV compared to 322 mV) and a smaller ΔE_p (168 mV compared to 195 mV), indicating a relatively higher reversibility of the reaction.

The quantitative determination of DOX was performed under optimal conditions. A range of increasing DOX concentrations (1.5 to 7.4 µmol L^{-1}) was used to establish the relationship between the concentration and the analytical signal, and this data was used for calibration curve construction. The sensitivity, LOD, and LOQ were also calculated from the calibration data.

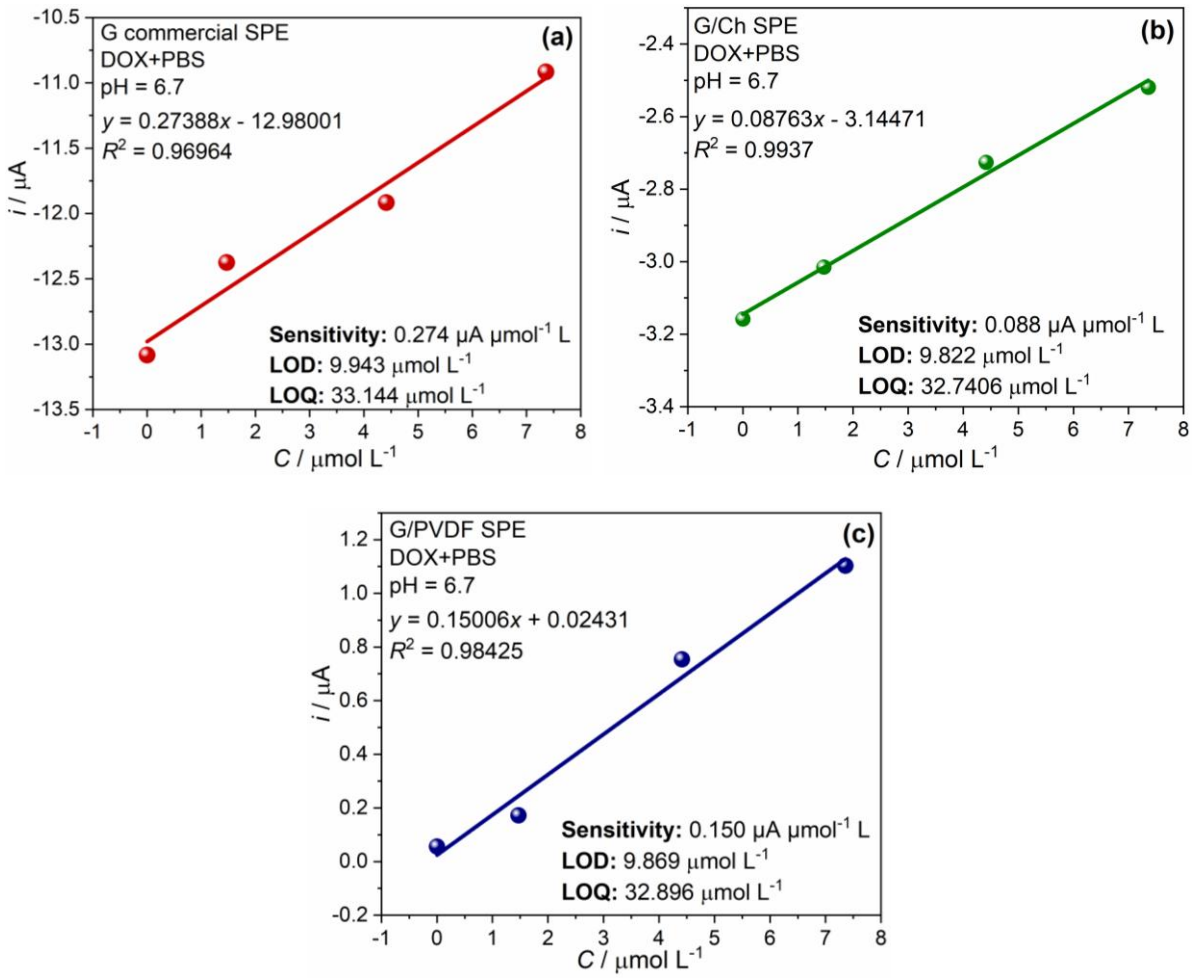

Figure 5. *Linear correspondence between the current and DOX's concentration for the (a) commercial graphene electrode; (b) chitosan-modified electrode and (c) PVDF-modified electrode*

Figure 5 illustrates the linear correlation between DOX concentration and the oxidation peak current for commercial and modified SPEs across various DOX concentrations. The modified electrodes exhibit strong linearity, with the chitosan-modified SPE showing the highest linear correlation, as described by $i_{ox.}$ = 0.08763*C* - 3.14471 (R^2 = 0.9937). The PVDF-modified electrode follows a linear equation of $i_{ox.}$ = 0.15006*C* + 0.02431 (R^2 = 0.98425). For comparison, the commercial, unmodified graphene SPE displays a linear relationship of $i_{ox.}$ = 0.27388*C* - 12.98001 (R^2 = 0.96964). These results highlight the improved electrochemical performance and linearity of the modified sensors, particularly the chitosan modification.

The sensitivity was determined to be 0.088 µA µmol^{-1} L for the chitosan-modified and 0.150 µA µmol^{-1} L for the PVDF-modified SPE, compared to a slope of 0.274 µA µmol^{-1} L for the commercial electrode. Additionally, LOD and LOQ were calculated within the same concentration range used for linear correlation. The chitosan-modified SPE achieved the lowest LOD and LOQ among the electrodes, with values of 9.822 and 32.7406 µmol L^{-1}, respectively. For the PVDF-modified SPE, the

LOD and LOQ were calculated to be 9.869 and 32.896 µmol L^{-1}, respectively, showing moderate sensitivity compared to the chitosan-modified electrode. The commercial electrode had the highest LOD and LOQ values, at 9.943 and 33.144 µmol L^{-1}, respectively. The results focus on the chitosan-modified SPE exhibiting the lowest detection and quantification limits, indicating its superior sensitivity among the tested electrodes.

Kinetic analysis and electrochemical mechanism determination of DOX's oxidation

Cyclic voltammograms scanned at different scan rates can usually be used for kinetic analysis of the oxidation process of DOX. The dependence of the current density at the oxidation peak $P_{ox.}$ on the scan rate can serve as a criterion for determining the reaction mechanism, specifically to identify the slow step of DOX oxidation, known as the rate-determining step. This helps to determine whether the reaction is controlled by an adsorption or a diffusion process of the reactants participating in the reaction. Figure 6 shows the voltammograms for both the commercial and polymer-modified SPEs.

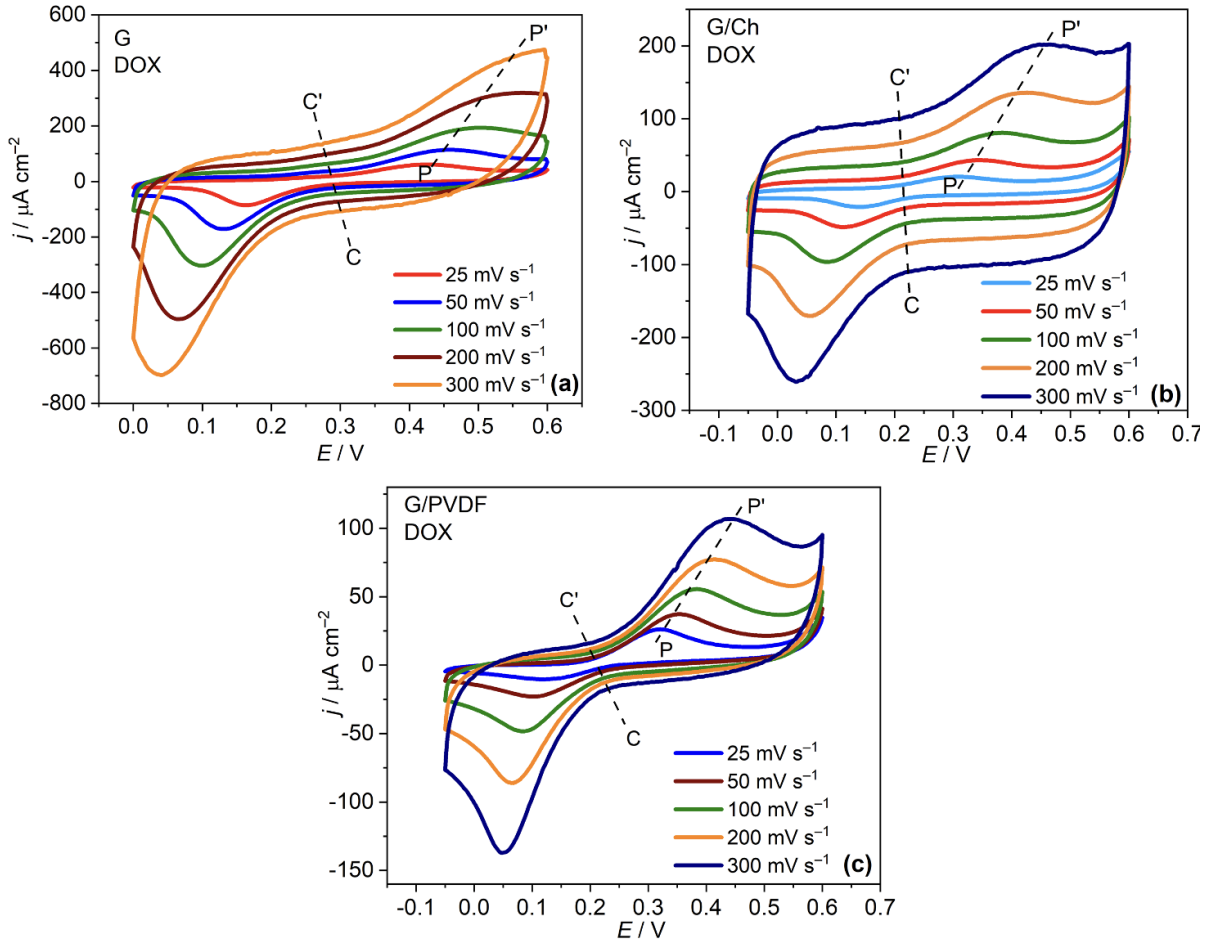

***Figure 6**. Cyclic voltammograms scanned at various scan rates for scan rate influence and kinetic analysis of the oxidation process of DOX onto (a) commercial G; (b) G/Ch and (c) G/PVDF modified electrode surface*

As the scan rate increases while testing the electrodes, the current density of all peaks increases. Moreover, the corresponding oxidation peak potentials shift towards the anodic direction (positive potential), while the reduction peaks shift towards the cathodic direction (negative potential).

The criteria for determining the rate-determining step of the electrochemical oxidation of DOX could be $j_{P_{ox.}}$ *vs.* v, $j_{P_{ox.}}$ *vs.* $v^{1/2}$, and log $j_{P_{ox.}}$ *vs.* log v plots are derived from the cyclic voltammograms shown in Figure 5 at the intersection line P-P'. The most eligible and confident criterion is the

log $j_{P_{Ox.}}$ *vs.* log *v* plot [62,63]. The value of the linear slope is the criterion for the rate-determining step of the reaction. If it is less than 0.5, the rate-determining step is the diffusion of the reactants, and if it is greater than 0.5, then the rate-determining step is adsorption [62,64]. The plots and the calculation for the limiting step are presented in Figure 7.

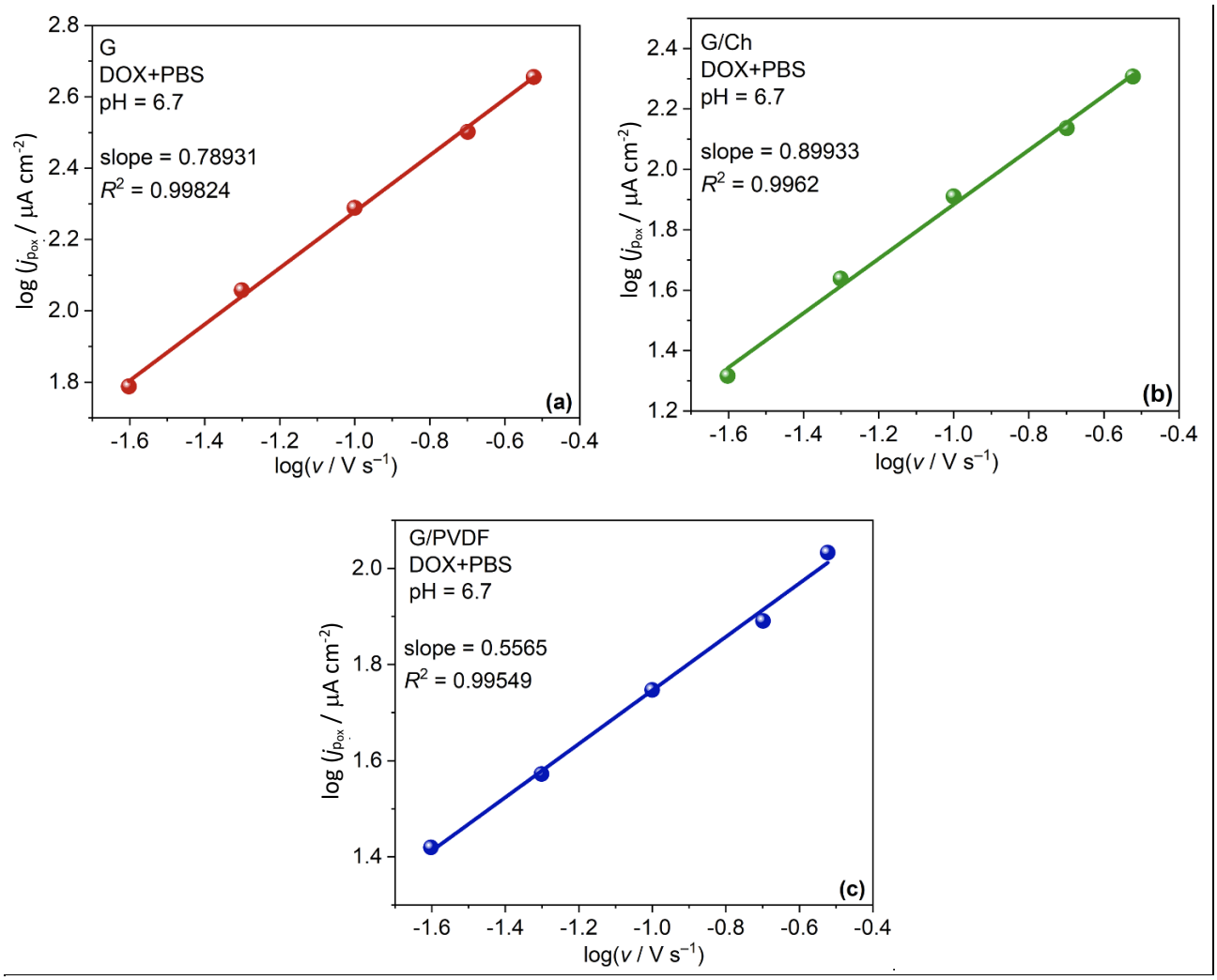

Figure 7. *Linear dependence of log* $j_{Pox.}$ *vs. log* v *for (a) commercial G; (b) G/Ch and (c) G/PVDF SPEs*

The linear dependence of all three plots is characterized by a very high correlation (>0.99). The slope for the commercial graphene and the chitosan-modified electrode has a calculated value of 0.789 (Figure 7a) and 0.899 (Figure 7b), respectively, unambiguously indicating that the rate-determining step of both processes is adsorption [65]. The PVDF-modified SPE has a slope value of 0.556 (Figure 7c), slightly higher than the boundary criterion, implying an adsorption or mixed control process [66,67].

The linear dependence between the potential ($E_{P_{Ox}}$) of the oxidation current maximum ($P_{Ox.}$) and the logarithm of the scan rate (log *v*) can be used to determine the electrochemical mechanism of the process, such as Tafel slope (*b*) and the number of exchanged electrons (*n*). The Tafel slope can be calculated using the Eq. (1) and (2) [68,69]:

$$E_{P_{Ox}} = \frac{b}{2}\log v + \text{const.} \quad (1)$$

$$\frac{dE_{P_{Ox}}}{d\log v} = \frac{b}{2} \quad (2)$$

The constant term (const.) in Eq. 1 represents the integration constant, as this equation describes the integral relationship between the oxidation potential (E_{Pox}) and the logarithm of the scan rate (log *v*). In Eq. (2), which depicts the differential form of this relationship, the constant term is not applicable and has been removed to reflect the correct mathematical representation.

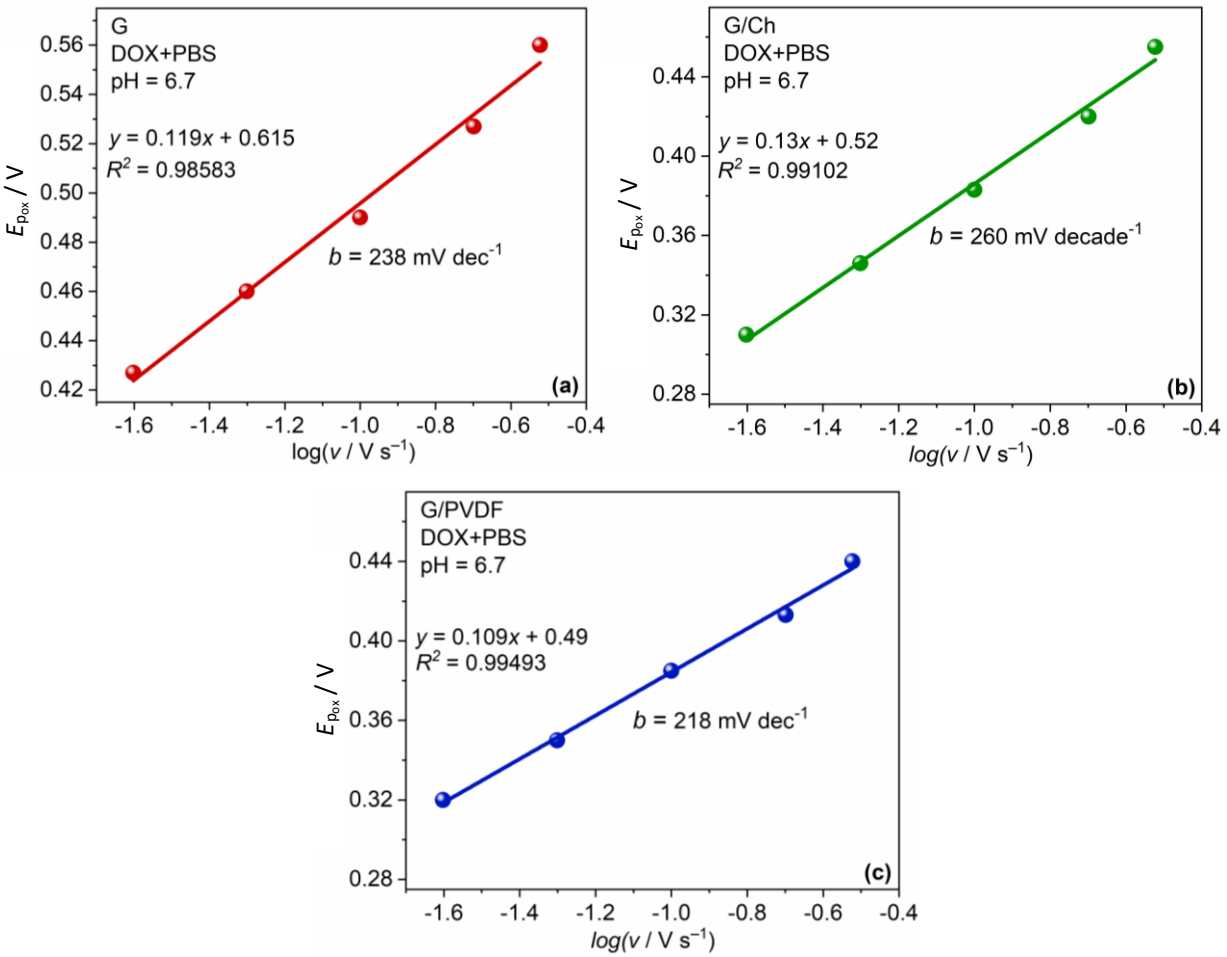

***Figure 8**. Linear dependence of E_{Pox} vs. logv (a) commercial G; (b) G/Ch and (c) G/PVDF SPE*

Figure 8 presents the E_{Pox} and log *v* dependence for the studied systems and the linear equation for each system is given in the plots. Tafel's slope values calculated using the data from the plots are 238 mV dec^{-1} for the commercial graphene, 260 mV dec^{-1} for the chitosan-modified, and 218 mV dec^{-1} for the PVDF-modified SPE. The values are shown in Table 1.

To calculate the number of transferred electrons, *n*, firstly, the charge transferred, *q*, needs to be calculated using the Eq. (3) [63]:

$$q = \frac{2.303\ k_B T}{b\alpha} \tag{3}$$

where k_B is the Boltzmann constant (1.38×10^{-23} J K^{-1}) and *T* is the temperature of 298 K. The electron transfer coefficient, *α*, can be calculated using the Eq. (4) [70]:

$$\alpha = \frac{2.303RT}{bF} \tag{4}$$

where *R* is the universal gas constant (8.134 J K^{-1} mol^{-1}), and *F* is the Faraday constant (96485 C mol^{-1}). Finally, the number of transferred electrons, *n*, was calculated using the Eq. (5):

$$n = \frac{q}{1.6\times10^{-19}} \tag{5}$$

where the value 1.6×10^{-19} corresponds to the charge of one electron. The electrochemical oxidation of DOX involves an exchange of one electron for all three systems. All calculated values are shown in Table 1. The estimated values for the Tafel slope of graphene SPEs correlate with the literature data for the electrochemical oxidation of DOX in the range between 210 and 260 mV dec^{-1} [71]. These values indicate that the one-electron transfer process is the determining step in the electrochemical oxidation of DOX for all studied systems.

***Table 1**. Electrochemical parameters (Tafel slope (b), electron transfer coefficient (α), number of transferred electrons (n)) calculated for all three studied systems*

Electrode	b / mV dec^{-1}	α	n
G	238	0.25	1
G/Ch	260	0.23	1
G/PVDF	218	0.27	1

Double-layer capacitance

The double-layer capacitance (C_{dl}) is intricately linked to the actual surface area of the electrodes. It can be calculated from the cyclic voltammograms shown in Figure 6. At the intersection C-C', in the region where the electrochemical double layer charge and discharge, a log C_{dl} *vs. v* plot can be derived. C_{dl} can be calculated using Eq. (6) [72]:

$$C_{dl} = \frac{dj_{cap.}}{d\left(\frac{\partial E}{\partial t}\right)} = \frac{dj_{cap.}}{v} \tag{6}$$

where E is the potential, v is the scan rate and $j_{cap.}$ is the capacitance current density, calculated as the average value of the absolute values of the anodic and cathodic currents densities at the C-C' intersection potential points, or following Eq. (7):

$$j_{cap.} = \frac{|j_{cat.}| + |j_{anod.}|}{2} \tag{7}$$

The change of the capacitance current density with the scan rate ($j_{cap.}$ *vs. v*) exhibits a strong linear dependence, as presented in Figure 9.

The slope of this linear dependence determines the double-layer capacity, C_{dl}, summarized in Table 2.

Table 2. Double-layer capacitance calculated values for the studied systems

Electrode	C_{dl} / mF cm^{-2}
G	0.384
G/Ch	0.338
G/PVDF	0.046

The commercial G electrode exhibits the highest double-layer capacitance of 0.384 mF cm^{-2}, indicating the greatest surface roughness (largest active surface), as confirmed by the SEM analysis. However, the capacitance decreases after the electrode is coated with either chitosan or PVDF, with the values calculated as 0.338 and 0.046 mF cm^{-2}, respectively. In the case of the chitosan-modified SPE, the reduction in capacitance is not significant. It is somewhat comparable to the commercial electrode, while it is more pronounced for the one modified with PVDF. The addition of PVDF to the surface results in graphene flakes being visibly covered with polymer clusters in the form of spherical particles.

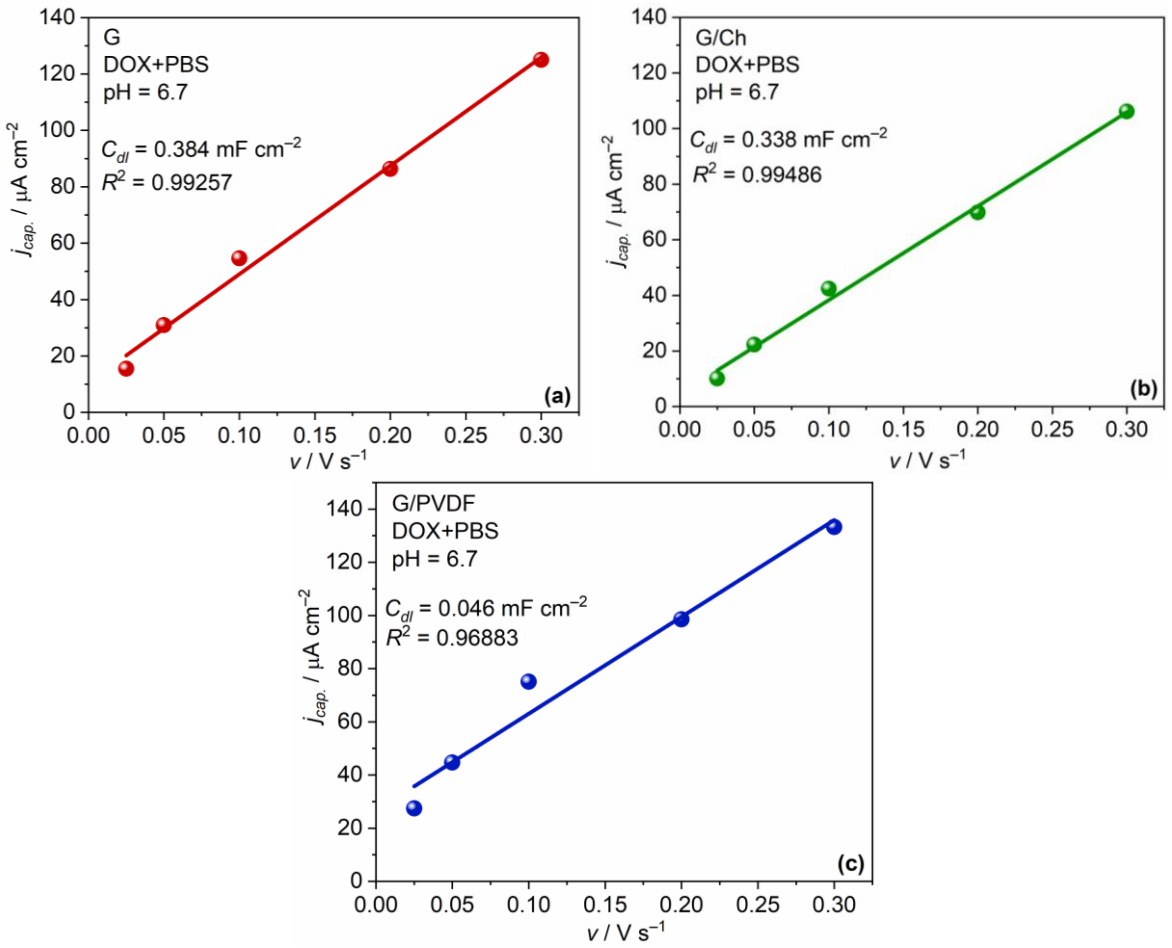

Figure 9. *Dependence of the capacitance current density on the scan rate ($j_{cap.}$ vs. v) for the (a) commercial G, (b) G/Ch, and (c) G/PVDF SPE*

The PVDF spherical particles appear to surround the graphene, filling the vacancies and leading to reduced surface porosity. This suggests a substantial reduction in surface roughness upon PVDF incorporation.

Repeatability, stability and reproducibility

The repeatability of the modified electrochemical sensors' response was assessed using 10 consecutive CV measurements to detect 0.002 mol L^{-1} DOX in 0.1 mol L^{-1} PBS at pH 6.7. The relative standard deviation (RSD) values obtained for triplicate experiments were 3.6 % for the chitosan-modified and 4.9 % for the PVDF-modified SPE, indicating reliable repeatability. Sensor stability was further evaluated by recording CV signals of 0.002 mol L^{-1} DOX over seven days. After one week, the chitosan-modified electrode exhibited a 10.2 % decrease in oxidation peak current from the initial values, demonstrating good long-term stability. The PVDF-modified SPE retained 86.0 % of its initial current response over the same period. After each use, the SPEs were rinsed thoroughly with 0.1 mol L^{-1} PBS and distilled water and then air-dried at room temperature. These results highlight the stability of the modifications, reflecting not only strong analytical performance but also enhanced physical protection of the working electrode. The findings suggest that, with appropriate handling, these electrodes can be reused despite the manufacturer Metrohm DropSens recommending them as disposable, single-use platforms for optimal performance. Reproducibility, indicating the precision of the modified electrodes, was investigated by testing three separate electrodes from each modification for 0.002 mol L^{-1} DOX detection, resulting in RSD values of 4.1 %

and 5.0 % for the chitosan and PVDF-modified SPE, respectively. These findings confirm that both modifications provide stable and repeatable measurements for DOX detection.

Physical characterization

SEM was used as a powerful visual technique to obtain detailed information about the electrodes' morphology and surface characteristics. The micrographs shown in Figure 10 present the commercial (10a and 10b), PVDF (10c and 10d), and Ch-modified (10e and 10f) graphene electrodes, respectively.

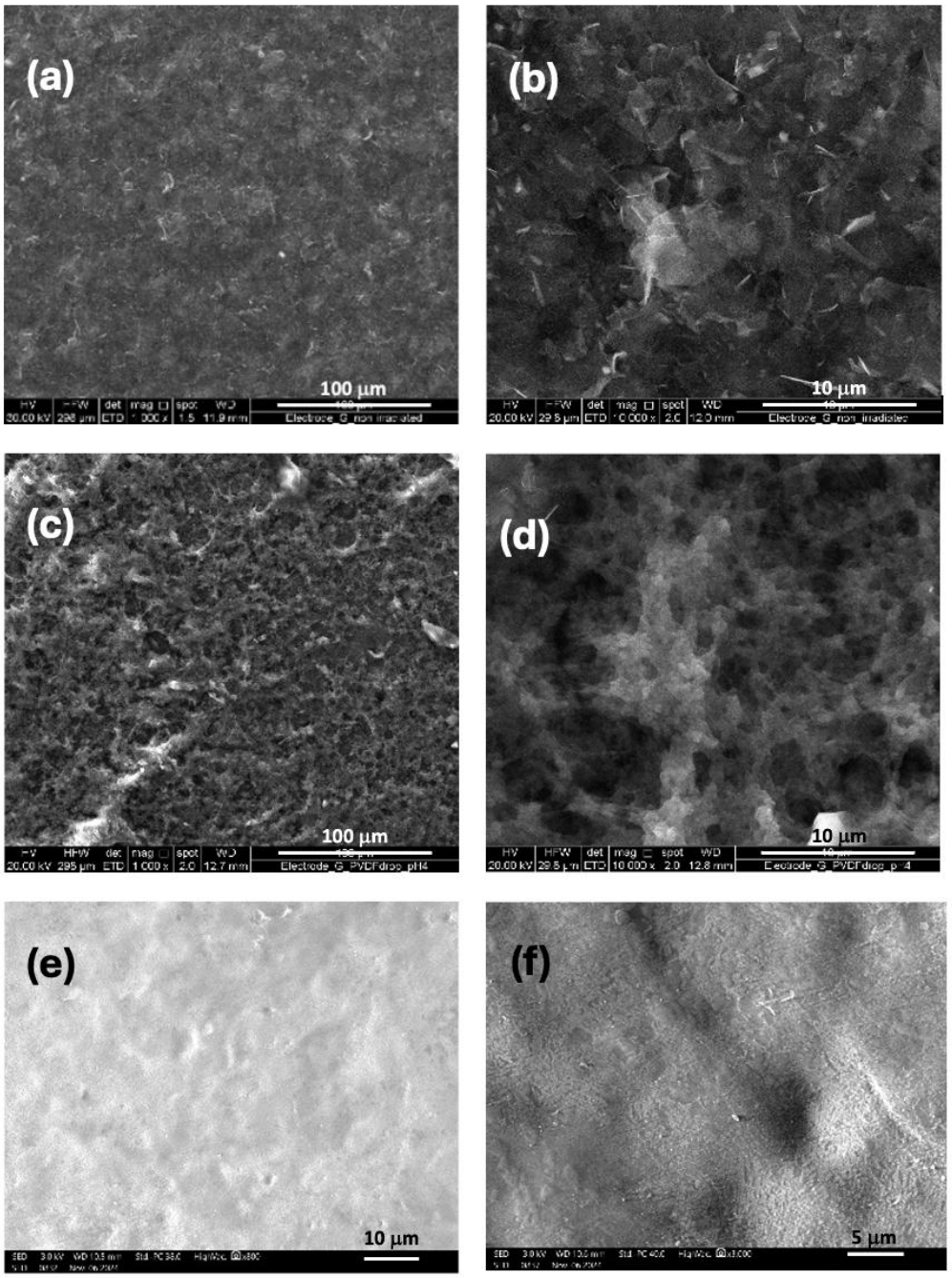

***Figure 10**. SEM micrographs of a commercial G electrode under (a) 1000× and (b) 10 000× magnification, PVDF-modified electrode under (c) 1000× and (d) 10 000× magnification, and chitosan-modified electrode under (e) 800× and (f) 6000× magnification*

The micrographs of the commercial SPE observed with a magnification of 1000× (Figure 10a) and 10000× (Figure 10b) depict the characteristic structure of the graphene, revealing layers of graphene

flakes with irregular structure and random orientation. This results in a working electrode with a rough surface and a large active area, two strongly favorable properties in the electrochemical sensor design. The micrographs of the PVDF-modified graphene electrode under magnification of 1000× (Figure 10c) and 10000× (Figure 10d) reveal the fibrous structure of the polymer film. PDVF's deposition onto the electrode's surface adds porosity upon evaporation of the solvent, contributing to a larger active area and a better response while detecting the analyte, thus enhancing the sensor's performance. The chitosan-modified graphene SPE demonstrates a uniform and continuous polymer film, as shown in the micrographs in Figures 10e and 10f. The chitosan coating fully covers the rough graphene surface, conforming closely to its heterogeneous morphology, indicating a strong interaction between the chitosan film and the graphene substrate. The microroughness observed in the micrograph taken at higher magnification provides potential adsorption sites, enhancing the electrode's effectiveness in detecting DOX. This morphology supports the interaction mechanism based on adsorption, highlighting the superiority of this electrode for DOX detection.

The electrolyte solution used for the CV measurements (0.002 mol L^{-1} DOX in 0.1 mol L^{-1} PBS, pH 6.7) was studied using ultraviolet-visible (UV-Vis) spectroscopy. The absorbance measurements and their corresponding spectra before and after exposing the electrolyte to the voltammetric measurements (to at least nine consecutive measurements - three electrodes tested in triplicates) are given in Figure 11. The analysis suggests that the electrolyte solution undergoes changes induced by the current when the electrochemical response is monitored through cyclic voltammetry. A current-induced change in the absorption of the solution at a wavelength of 482 nm was noted as a decrease from 2.75 to 1.58. While DOX generally undergoes reversible redox processes (discussed in the Electrochemical detection part), the observed decrease in absorption could indicate partial or temporary adsorption of DOX onto the electrode surface, resulting in lower solution concentration. This absorption correlates to the interaction mechanism of DOX with the SPE. For further clarification, the maximal absorbance wavelengths for both redox forms of DOX are 485 nm for the oxidized and 480 to 490 nm for the reduced form, depending on the environmental conditions [73-75]. The maximal excitation noted in Figure 11 corresponds to the DOX's oxidized form rather than the product of reduction - doxorubicinol.

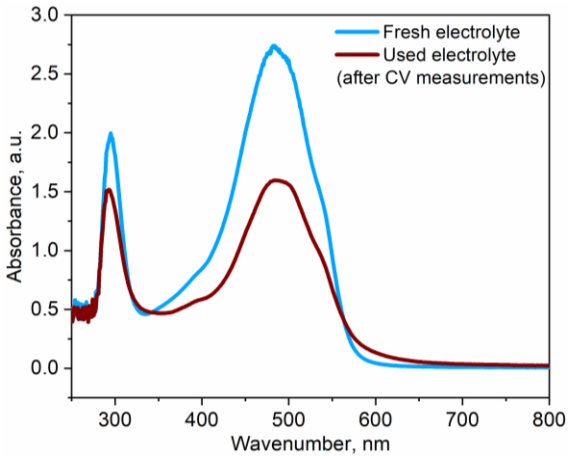

***Figure 11**. UV-Vis spectra of 0.1M PBS solution (pH 6.7)*

Conclusions

Simple electrochemical sensors based on screen-printed graphene electrodes were applied to detect a chemotherapy medication, doxorubicin hydrochloride, in a simulated biological environment with pH 6.7. While studies in the literature contribute to the field, no other researcher investigated the proposed polymer-modified sensor, underscoring its novelty. Our simple design

approach consists of a screen-printed electrode platform, modified by drop deposition of chitosan and PVDF as thin polymeric films onto the electrode's surface. The electrochemical reactivity and performance of the electrodes were tested and compared to the commercial graphene SPE using cyclic voltammetry. The presence of DOX in the solutions induced characteristic redox peaks in the voltammograms and led to the appearance of a reversible reaction. Polymer-modified graphene electrodes exhibited a broad current intensity and achieved the desired rectangular form in the voltammograms due to their exceptional electrical properties. The electrochemical behavior confirmed that both modified electrodes displayed excellent electrochemical properties for the determination and monitoring of DOX, with a promising application in the field of pharmaceutical drug detection. However, according to the thoroughly conducted electrochemical analysis, the chitosan-modified electrode exhibits superior properties compared to the PVDF-modified one, such as lower $P_{ox.}$, higher reversibility, lower LOD and LOQ, and higher double-layer capacitance *i.e.,* larger active surface area. The electrodes demonstrated excellent repeatability, stability, and reproducibility, confirming their suitability for sensitive DOX detection. The simplicity and cost-effectiveness of the polymer-modified screen-printed electrodes make them promising candidates for pharmaceutical drug analysis and on-site in vivo diagnostics.

Conflict of interest: *The authors declare no conflict of interest.*

References

[1] C. Carvalho, R. X. Santos, S. Cardoso, S. Correia, P. J. Oliveira, M. S. Santos, P. I. Moreira, Doxorubicin: the good, the bad and the ugly effect, *Current Medicinal Chemistry* **16(25)** (2009) 3267-3285 https://doi.org/10.2174/092986709788803312.

[2] G. Minotti, S. Recalcati, A. Mordente, G. Liberi, A. M. Calafiore, C. Mancuso, P. Preziosi, G. Cairo, The secondary alcohol metabolite of doxorubicin irreversibly inactivates aconitase/iron regulatory protein-1 in cytosolic fractions from human myocardium. *Federation of American Societies for Experimental Biology Journal* **12(7)** (1998) 541-52 https://doi.org/10.1096/fasebj.12.7.541.

[3] M. A. Mitry, J. G. Edwards, Doxorubicin induced heart failure: Phenotype and molecular mechanisms, *International Journal of Cardiology Heart & Vasculature* **10(17-24)** (2016) 17-24 http://doi.org/10.1016/j.ijcha.2015.11.004.

[4] J. H. Beijnen, P. L. Meenhorst, R. Van Gijn, M. Fromme, H. Rosing, W. J. M. Underberg, HPLC determination of doxorubicin, doxorubicinol and four aglycone metabolites in plasma of AIDS patients, *Journal of Pharmaceutical and Biomedical Analysis* **9(10-12)** (1991) 995-1002 https://doi.org/10.1016/0731-7085(91)80036-9.

[5] K. Alhareth, C. Vauthier, C. Gueutin, G. Ponchel, F. Moussa, HPLC quantification of doxorubicin in plasma and tissues of rats treated with doxorubicin loaded poly(alkylcyanoacrylate) nanoparticles, *Journal of Chromatography B* **887-888** (2012) 128-132 https://doi.org/10.1016/j.jchromb.2012.01.025.

[6] S. Ahmed, N. Kishikawa, K. Ohyama, M. Wada, K. Nakashima, N. Kuroda, Selective determination of doxorubicin and doxorubicinol in rat plasma by HPLC with photosensitization reaction followed by chemiluminescence detection, *Talanta*, **78(1)** (2009) 94-100 https://doi.org/10.1016/j.talanta.2008.10.043.

[7] C. Mazuel, J. Grove, G. Gerin, K. P. Keenan, HPLC-MS/MS determination of a peptide conjugate prodrug of doxorubicin, and its active metabolites, leucine-doxorubicin and doxorubicin, in dog and rat plasma, *Journal of Pharmaceutical and Biomedical Analysis*, **33(5)** (2003) 1093-1102 https://doi.org/10.1016/S0731-7085(03)00434-5.

[8] A. S. Rodrigues and others, Development of an Analytical Methodology for Simultaneous Determination of Vincristine and Doxorubicin in Pharmaceutical Preparations for Oncology by HPLC—UV, *Journal of Chromatographic Science*, **47(5)** 387-391 https://doi.org/10.1093/chromsci/47.5.387.

[9] E. Configliacchi, G. Razzano, V. Rizzo, A. Vigevani, HPLC methods for the determination of bound and free doxorubicin, and of bound and free galactosamine, in methacrylamide polymer-drug conjugates,

Journal of Pharmaceutical and Biomedical Analysis, **15(1)** (1996) 123-129 https://doi.org/10.1016/0731-7085(96)01825-0.

[10] Q. Zhou, B. Chowbay, Determination of doxorubicin and its metabolites in rat serum and bile by LC: application to preclinical pharmacokinetic studies, *Journal of Pharmaceutical and Biomedical Analysis*, **30(4)** (2002), 1063-1074 https://doi.org/10.1016/S0731-7085(02)00442-9.

[11] W. Ma, J. Wang, Q. Guo, P. Tu, Simultaneous determination of doxorubicin and curcumin in rat plasma by LC-MS/MS and its application to pharmacokinetic study, *Journal of Pharmaceutical and Biomedical Analysis* **111** (2015) https://doi.org/10.1016/j.jpba.2015.04.007.

[12] Y. Xie, N. Shao, Y. Jin, L. Zhang, H. Jiang, N. Xiong, F. Su, H. Xu, Determination of non-liposomal and liposomal doxorubicin in plasma by LC-MS/MS coupled with an effective solid phase extraction: In comparison with ultrafiltration technique and application to a pharmacokinetic study, *Journal of Chromatography B* **1072** (2018) 149-160 https://doi.org/10.1016/j.jchromb.2017.11.020.

[13] M. Janicka, A. Kot-Wasik, J.Paradziej-Łukowicz, G. Sularz-Peszyńska, A. Bartoszek, J. Namieśnik, LC-MS/MS Determination of Isoprostanes in Plasma Samples Collected from Mice Exposed to Doxorubicin or Tert-Butyl Hydroperoxide, *International Journal of Molecular Sciences* **14(3)** (2013) 6157-6169 https://doi.org/10.3390/ijms14036157.

[14] C. Bobin-Dubigeon and others, A New, Validated Wipe-Sampling Procedure Coupled to LC-MS Analysis for the Simultaneous Determination of 5-Fluorouracil, Doxorubicin and Cyclophosphamide in Surface Contamination, *Journal of Analytical Toxicology* **37(7)** (2013) 433-439 https://doi.org/10.1093/jat/bkt045.

[15] S. Mazzucchelli, A. Ravelli, F. Gigli, M. Minoli, F. Corsi, P. Ciuffreda, R. Ottria, LC-MS/MS method development for quantification of doxorubicin and its metabolite 13-hydroxy doxorubicin in mice biological matrices: Application to a pharmaco-delivery study, *Biomedical Chromatography* **31(4)** 2017 https://doi.org/10.1002/bmc.3863.

[16] I. Dimitrievska, P. Paunovic, A. Grozdanov, Recent advancements in nano sensors for air and water pollution control, *Material Science and Engineering* **7(2)** (2023) 113–128 https://doi.org/10.15406/mseij.2023.07.00214.

[17] M. Hossein Ghanbari, Z. Norouzi, A new nanostructure consisting of nitrogen-doped carbon nanoonions for an electrochemical sensor to the determination of doxorubicin, *Microchemical Journal* **157(9)** (2020) https://doi.org/10.1016/j.microc.2020.105098.

[18] I. M. Apetrei, C. Apetrei, Voltammetric determination of melatonin using a graphene-based sensor in pharmaceutical products, *International Journal of Nanomedicine* **11** (2016) 1859-1866 https://doi.org/10.2147/IJN.S104941.

[19] J. Soleymani, M. Hasanzadeh, M. Eskandani, M. Khoubnasabjafari, N. Shadjou, A. Jouyban, Electrochemical sensing of doxorubicin in unprocessed whole blood, cell lysate, and human plasma samples using thin film of poly-arginine modified glassy carbon electrode, *Materials Science and Engineering: C* **77** (2017) 790-802 https://doi.org/10.1016/j.msec.2017.03.257.

[20] I. A. Mattioli, P. Cervini, É. T. G. Cavalheiro, Screen-printed disposable electrodes using graphite-polyurethane composites modified with magnetite and chitosan-coated magnetite nanoparticles for voltammetric epinephrine sensing: a comparative study, *Microchimica Acta* **187(6)** (2020) https://doi.org/10.1007/s00604-020-04259-x.

[21] N. A. Negm, H. A. Abubshait, S. A. Abubshait, M. T. H. Abou Kana, E. A. Mohamed, M. M. Betiha, Performance of chitosan polymer as platform during sensors fabrication and sensing applications, *International Journal of Biological Macromolecules* **165** (2020) 402-435 https://doi.org/10.1016/j.ijbiomac.2020.09.13.

[22] R. Dallaev, T. Pisarenko, D. Sobola, F. Orudzhev, S. Ramazanov, T. Trčka, Brief Review of PVDF Properties and Applications Potential, *Polymers* **14(22)** (2022) 4793 https://doi.org/10.3390/polym14224793.

[23] M. Sobhy, R. M. Khafagy, A. A. Soliman, *et al*., Design of Biosensor Based on Graphene Oxide/ WO3/ Polyvinylidene Fluoride, *Optical and Quantum Electronics* **55** (2023) 789 https://doi.org/10.21203/rs.3.rs-2710142/v1.

[24] H. Zhao, K. Shi, C. Zhang, J. Ren, M. Cui, N. Li, X. Ji, R. Wang, Spherical COFs decorated with gold nanoparticles and multiwalled carbon nanotubes as signal amplifier for sensitive electrochemical

detection of doxorubicin, *Microchemical Journal* **182** (2022) https://doi.org/10.1016/j.microc.2022.107865.

[25] M. Mehmandoust, Y. Khoshnavaz, F. Karimi, S. Çakar, M. Özacar, N. Erk, A novel 2-dimensional nanocomposite as a mediator for the determination of doxorubicin in biological samples, *Environmental Research* **213** (2022) https://doi.org/10.1016/j.envres.2022.113590.

[26] M. Abbasi, M. Ezazi, A. Jouyban, E. Lulek, K. Asadpour-Zeynali, Y. Nuri Ertas, J. Houshyar, A. Mokhtarzadeh, A. Soleymani, An ultrasensitive and preprocessing-free electrochemical platform for the detection of doxorubicin based on tryptophan/polyethylene glycol-cobalt ferrite nanoparticles modified electrodes, *Microchemical Journal* **183** (2022) https://doi.org/10.102916/j.microc.2022.108055.

[27] H. Guo, H. Jin, R. Gui, Z. Wang, J. Xia, F. Zhang, Electrodeposition one-step preparation of silver nanoparticles/carbon dots/reduced graphene oxide ternary dendritic nanocomposites for sensitive detection of doxorubicin, *Sensors and Actuators B: Chemical* **253** (2017) 50-57 https://doi.org/10.1016/j.snb.2017.06.095.

[28] D. M. Stanković, Z. Milanović, L. Švorc, V. Stanković, D. Janković, M. Mirković, S. Vranješ Đurić, Screen printed diamond electrode as efficient "point-of-care" platform for submicromolar determination of cytostatic drug in biological fluids and pharmaceutical product, *Diamond and Related Materials* **113** (2021) https://doi.org/10.1016/j.diamond.2021.108277

[29] M. Behravan, H. Aghaie, M. Giahi, L. Maleknia, Determination of doxorubicin by reduced graphene oxide/gold/polypyrrole modified glassy carbon electrode: A new preparation strategy, *Diamond and Related Materials* **117** (2021) https://doi.org/10.1016/j.diamond.2021.108478.

[30] N. Thakur, V. Sharma, T. Abhishek Singh, A. Pabbathi, J. Das, Fabrication of novel carbon dots/cerium oxide nanocomposites for highly sensitive electrochemical detection of doxorubicin, *Diamond and Related Materials* **125** (2022) https://doi.org/10.1016/j.diamond.2022.109037.

[31] T. Abhishek Singh, V. Sharma, N. Thakur, N. Tejwan, A. Sharma, J. Das, Selective and sensitive electrochemical detection of doxorubicin via a novel magnesium oxide/carbon dot nanocomposite based sensor, *Inorganic Chemistry Communications* **150** (2023) https://doi.org/10.1016/j.inoche.2023.110527.

[32] S. Sun, X. Xu, N. Aiu, Z. Sun, Y. Zhai, S. Li, C. Xuan, Y. Zhou, X. Yang, T. Zhou, Q. Tian, Novel Electrochemical Sensor Based on Acetylene Black for the Determination of Doxorubicin in Serum Samples, *International Journal of Electrochemical Science* **17** (2022) https://doi.org/10.20964/2022.11.82.

[33] J. Sharifi, H. Fayazfar, Highly sensitive determination of doxorubicin hydrochloride antitumor agent via a carbon nanotube/gold nanoparticle based nanocomposite biosensor, *Bioelectrochemistry* **139** (2021) https://doi.org/10.1016/j.bioelechem.2021.107741.

[34] A. R. Alavi-Tabari, A. Khalilzadeh, H. Karimi-Maleh, Simultaneous determination of doxorubicin and dasatinib as two breast anticancer drugs uses an amplified sensor with ionic liquid and ZnO nanoparticle, *Journal of Electroanalytical Chemistry* **811** (2018) 84-88 https://doi.org/10.1016/j.jelechem.2018.01.034.

[35] E. M. Materon, A. Wong, O. Fatibello-Filho, R. Censi Faria, Development of a simple electrochemical sensor for the simultaneous detection of anticancer drugs, *Journal of Electroanalytical Chemistry* **827** (2018) 64-72 https://doi.org/10.1016/j.jelechem.2018.09.010.

[36] M. Rahimi, G. Bagheri, S. Jamilaldin Fatemi, A new sensor consisting of bird nest-like nanostructured nickel cobaltite as the sensing element for electrochemical determination of doxorubicin, *Journal of Electroanalytical Chemistry* **848** (2019) https://doi.org/10.1016/j.jelechem.2019.113333.

[37] N. Hashemzadeh, M. Hasanzadeh, N. Shadjou, J. Eivazi-Ziaei, M. Khoubnasabjafari, A. Jouyban, Graphene quantum dot modified glassy carbon electrode for the determination of doxorubicin hydrochloride in human plasma, *Journal of Pharmaceutical Analysis* **6(4)** (2016) 235-241 https://doi.org/10.1016/j.jpha.2016.03.003.

[38] S. Zia Mohammadi, F. Mousazadeh, S. Tajik, Simultaneous Determination of Doxorubicin and Dasatinib by using Screen-Printed Electrode/Ni-Fe Layered Double Hydroxide, *Industrial & Engineering Chemistry Research* **62(11)** (2023) 4646-4654 https://doi.org/10.1021/acs.iecr.2c03105.

[39] I. Rus, M. Tertis, C. Barbˇalatˇa, A. Porfire, I. Tomutˇa, R. Sˇandulescu, C. Cristea, An Electrochemical Strategy for the Simultaneous Detection of Doxorubicin and Simvastatin for Their Potential Use in the Treatment of Cancer, *Biosensors* **11(15)** (2021) https://doi.org/10.3390/bios11010015.
[40] M. Wang, J. Lin, J. Gong, M. Ma, H. Tang, J. Liu, F. Yan, Rapid and sensitive determination of doxorubicin in human whole blood by vertically-ordered mesoporous silica film modified electrochemically pretreated glassy carbon electrodes, *Royal Society of Chemistry Advances* **11** (2021) 9021 https://doi.org/10.1039/d0ra10000e.
[41] Y. Guo, Y. Chen, Q. Zhao, S. Shuang, C. Dong, Electrochemical Sensor for Ultrasensitive Determination of Doxorubicin and Methotrexate Based on Cyclodextrin-Graphene Hybrid Nanosheets, *Electroanalysis* **23** (2011) 2400 - 2407 https://doi.org/10.1002/elan.201100259.
[42] C. Zhang, X. Zhou, F. Yan, J. Lin, N-Doped Graphene Quantum Dots Confined within Silica Nanochannels for Enhanced Electrochemical Detection of Doxorubicin *Molecules* **28** (2023) 6443 https://doi.org/10.3390/molecules28186443.
[43] E. Haghshenas, T. Madrakian, A. Afkhami, Electrochemically oxidized multiwalled carbon nanotube/glassy carbon electrode as a probe for simultaneous determination of dopamine and doxorubicin in biological samples, *Analytical and Bioanalytical Chemistry* **408** (2016) 2577-2586 https://doi.org/10.1007/s00216-016-9361-y.
[44] J. Fei, X. Wen, Y. Zhang, L. Yi, X. Chen, H. Cao Voltammetric determination of trace doxorubicin at a nano-titania/nafion composite film modified electrode in the presence of cetyltrimethylammonium bromide, *Microchimica Acta* **164** (2009) 85-91, https://doi.org/10.1007/s00604-008-0037-y.
[45] M. Taei, F. Hasanpour, H. Salavati, S. Mohammadian, Fast and sensitive determination of doxorubicin using multi-walled carbon nanotubes as a sensor and CoFe2O4 magnetic nanoparticles as a mediator, *Microchimica Acta* **183** (2016) 49-56, https://doi.org/10.1007/s00604-015-1588-3.
[46] S. Kummari, L. Panicker, K.V. Gobi, R. Narayan, Y.G. Kotagiri, Electrochemical Strip Sensor Based on a Silver Nanoparticle-Embedded Conducting Polymer for Sensitive In Vitro Detection of an Antiviral Drug, *ACS Applied Nano Materials* **6(13)** (2023) 12381-12392 https://doi.org/10.1021/acsanm.3c02080.
[47] G. Krishnaswamy, G. Shivaraja, S. Sreenivasa, Aruna Kumar D. B, Votammetric applications in Drug detection: Mini Review, *Volatmmetry for Sensing Applications* **11** (2022) 281-305 https://doi.org/10.2174/9789815039719122010013.
[48] S. Sadak, I. Atay, S. Kurbanoglu, B. Uslu, Disposable Electrochemical Sensors for Biomedical Applications, *ACS Recent Developments of Green Electrochemical Sensors* **1437(8)** (2023) 157-191 https://doi.org/10.1021/bk-2023-1437.ch008.
[49] Z. Bagheri Nasab, F. Garkani Nejad, Electrochemical Sensor Based on a Modified Graphite Screen Printed Electrode for Amitriptyline Determination, *Surface Engineering and Applied Electrochemistry* **58** (2022) 100-108 https://doi.org/10.3103/S1068375522010070.
[50] B. Bozal-Palabiyik, B. Dogan-Topal, S. A. Ozkan, B. Uslu, New trends in Electrochemical sensor modified with carbon nanotubes and graphene for pharmaceutical analysis, *Recent Advances in Analytical Techniques* **2** (2018) 249-301 https://doi.org/10.2174/9781681085746118020009.
[51] A. V. Bounegru, I. Bounegru, Chitosan-Based Electrochemical Sensors for Pharmaceuticals and Clinical Applications, *Polymers* **15(17)** (2023) 3539; https://doi.org/10.3390/polym15173539.
[52] S. Traipop, W. Jesadabundit, W. Khamcharoen, T. Pholsiri, S. Naorungroj, S. Jampasa, O. Chailapakul, Nanomaterial-based Electrochemical Sensors for Multiplex Medicinal Applications, *Current Topics in Medicinal Chemistry* **24(11)** (2024) 986 - 1009 https://doi.org/10.2174/0115680266304711240327072348
[53] M. Wang, J. Lin, J. Gong, M. Ma, H. Tang, J. Liu, F. Yan F, Rapid and sensitive determination of doxorubicin in human whole blood by vertically-ordered mesoporous silica film modified electrochemically pretreated glassy carbon electrodes, *Royal Society of Chemistry Advances* **11** (2021) 9021-9028 https://doi.org/10.1039/D0RA10000E.
[54] Y. Guo, Y. Chen, Q. Zhao, S. Shuang, C. Dong, Electrochemical Sensor for Ultrasensitive Determination of Doxorubicin and Methotrexate Based on Cyclodextrin-Graphene Hybrid Nanosheets, *Electroanalysis* **23(10)** (2011) 2400-2407 https://doi.org/10.1002/elan.201100259.
[55] J. Soleymani, M. Hasanzadeh, N. Shadjou, M. Khoubnasab Jafari, J. V. Gharamaleki, M. Yadollahi, A. Jouyban, A new kinetic-mechanistic approach to elucidate electrooxidation of doxorubicin

hydrochloride in unprocessed human fluids using magnetic graphene-based nanocomposite modified glassy carbon electrode, *Materials Science and Engineering: C* **61** (2016) 638-650 https://doi.org/10.1016/j.msec.2016.01.003.

[56] S. M. Ilies, B. Schinteie, A. Pop, S. Negrea, C. Cretu, E. I. Szerb, F. Manea, Graphene Quantum Dots and Cu(I) Liquid Crystal for Advanced Electrochemical Detection of Doxorubicin in Aqueous Solutions, *Nanomaterials* **11** (2021) 2788 https://doi.org/10.3390/nano11112788.

[57] F. Chekin, V. Myshin, R. Ye, S. Melinte, S. K. Singh, S. Kurungot, R. Boukherroub, S. Szunerits, Graphene-modified electrodes for sensing doxorubicin hydrochloride in human plasma, *Analytical and Bioanalytical Chemistry* **411** (2019) 1509-1516, https://doi.org/10.1007/s00216-019-01611-w.

[58] E. Hghshenas, T. Madrakian, A. Afkhami, Electrochemically oxidized multiwalled carbon nanotube/glassy carbon electrode as a probe for simultaneous determination of dopamine and doxorubicin in biological samples, *Analytical and Bioanalytical Chemistry* **408** (2019) 2577-2586 https://doi.org/10.1007/s00216-016-9361-y.

[59] P. Paunović, A. Grozdanov, I. Dimitrievska, A. Tomova, Voltammetric Detection of Diclofenac with Screen-printed Electrodes Based on Graphene and PVDF-Modified Graphene, *Chemistry in Industry* **73(7-8)** (2024) 293-302 https://doi.org/10.15255/KUI.2023.058.

[60] H. Imran, Y. Tang, S. Wang, X. Yan, C. Liu, L. Guo, E. Wang, C. Xu, Optimized DOX Drug Deliveries via Chitosan-Mediated Nanoparticles and Stimuli Responses in Cancer Chemotherapy: A Review, *Molecules* **29(1)** 2024 31 https://doi.org/10.3390/molecules29010031.

[61] I. M. Apetrei, C. Apetrei, Voltametric determination of melatonin using a graphene-based sensor in pharmaceutical products, *International Journal of Nanomedicine* **11** (2016) 1859-1866 http://doi.org/10.2147/IJN.S104941.

[62] R. C. Carvalho, A. J. Betts, J. F. Cassidy, Diclofenac determination using CeO2 nanoparticle modified screen-printed electrodes - A study of background correction, *Microchemical Journal* **158** (2020) 105258 https://doi.org/10.1016/j.microc.2020.105258.

[63] U. Ciltas, B. Yilmaz, S. Kaban, B. K. Akcay, G. Nazik, Study on the interaction between isatin-β-thiosemicarbazone and calf thymus DNA by spectroscopic techniques. *Iranian Journal of Pharmaceutical Research* **15** (2014) 715-722 https://doi.org/10.22037/ijpr.2015.1691.

[64] E. S. Gil, R. O. Couto, Flavonoid electrochemistry: a review on the electroanalytical applications, *Brazilian Journal of Pharmacognosy* **23** (2013) 542-558 https://doi.org/10.1590/S0102-695X2013005000031.

[65] J. A. Gothi Grace, A. Gomathi, C. Vedhi, Electrochemical behaviour of 1,4-diaminoanthra-9,10-quinone at conducting polymer based modified electrode, *Journal of Advanced Chemical Sciences* **2(3)** (2016) 366-368 ISSN: 2394-5311.

[66] S. Guan, X. Fu, B. Zhang, M. Lei, Z. Peng, Cation-exchange-assisted formation of NiS/SnS2 porous nanowalls with ultrahigh energy density for battery-supercapacitor hybrid devices, *Journal of Materials Chemistry A* **6** (2020) 3300-3310 https://doi.org/10.1039/C9TA11517J.

[67] G. A. J. Merghani, A. A. Elbashir, Development of chemically modified electrode using cucurbit(6)uril to detect ranitidine hydrochloride in pharmaceutical formulation by voltammetry, *Journal of Analytical and Pharmaceutical Research* **7** (2018) 634-639 https://doi.org/10.15406/japlr.2018.07.00294.

[68] H. Beitollahi, M. Hamzavi, M. Torkzadeh-Mahani, Electrochemical determination of hydrochlorothiazide and folic acid in real samples using a modified graphene oxide sheet paste electrode, *Materials Science and Engineering: C* **52** (2015) 297-305 https://doi.org/10.1016/j.msec.2015.03.031.

[69] W. He, Y. Ding, W. Zhang, L. Ji, X. Zhang, F. Yang, A highly sensitive sensor for simultaneous determination of ascorbic acid, dopamine and uric acid based on ultra-small Ni nanoparticles, *Journal of Electroanalytical Chemistry* **775** (2016) 205-211 https://doi.org/10.1016/j.jelechem.2016.06.001.

[70] P. Paunović, A. Grozdanov, I. Dimitrievska, M. Paunović, M. Mitevska, *Sofia Electrochemical Days, Irradiation Treatment on Sensing Performances of Screen-Printed Electrodes Aimed for Monitoring of Anticancer Drug - Doxorubicin*, Varna, Bulgaria, 2024, p. 14.

[71] E. Gileadi, *Electrode Kinetics for Chemists, Chemical Engineers, and Materials Scientists*, VCH Publishers Inc., New York, USA, 1993, ISBN: 978-0-471-18858-2.

[72] L. M. Silva, L. A. Faria, J. F. C. Boodts, Determination of the morphology factor of oxide layers, *Electrochimica Acta* **47** (2001) 395-403 https://doi.org/10.1016/S0013-4686(01)00738-1.
[73] Y. Chen, Y. Zhang, Z. Wu, X. Peng, T. Su, J. Cao, B. He, S. Li, Biodegradable poly(ethylene glycol)-poly(ε-carprolactone) polymeric micelles with different tailored topological amphiphilies for doxorubicin (DOX) drug delivery, *Royal Society of Chemistry Advances* **63** (2016) http://doi.org/10.1039/C6RA06040D.
[74] J. Liang, Z. Zhang, H. Zhao, S. Wan, X. Zhai, J. Zhou, R. Liang, Q. Deng, Y. Wu, G. Lin, Simple and rapid monitoring of doxorubicin using streptavidin-modified microparticle-based time-resolved fluorescence immunoassay, *Royal Society of Chemistry Advances* **8** (2018) 15621-15631 https://doi.org/10.1039/C8RA01807C.
[75] R. Bartzatt, E. Weidner, Analysis for doxorubicin by spectrophotometry and reversed phase high performance liquid chromatography (HPLC), *Current Topics in Analytical Chemistry* **9** (2012) 63-69 (PDF) Analysis for doxorubicin by spectrophotometry and reversed phase high performance liquid chromatography (HPLC)